

Supplementary information for

Coulomb explosion of vertically aligned carbon nanofibre induced by field electron emission

Yunhan Li^a, Yonghai Sun^{a, b}, David A. Jaffray^b, and John T. W. Yeow^{a, *}

^a Department of Systems Design Engineering, University of Waterloo, 200 University Ave. West, Waterloo, Ontario, Canada, N2L 3G1

^b Princess Margaret Cancer Centre, 610 University Ave, Toronto, ON, Canada, M5G 2M9

* Email: jyeow@uwaterloo.ca

1. Uniformity of carbon nanofibre (CNF) field emitters' height
2. Experimental validation of CNF explosion
3. Energy-dispersive X-ray spectroscopy analysis of the explosion site
4. Tubular cone structure of CNF emitters
5. Supplementary videos

References

1. Uniformity of carbon nanofibre (CNF) field emitters' height

Fig. S1(a) shows a typical CNF field emitter array (FEA) using the same synthesise process as the 11×11 CNF FEA. The CNF emitters have an average height of 5.12 μm and a standard deviation of 0.55 μm , which is 10.7% of the average. The data of CNF emitters' height uniformity is in good agreement with that reported in the previous study (6.3%). Fig. S1(b) shows the distribution in CNF emitters' heights and Gaussian distribution fitting.

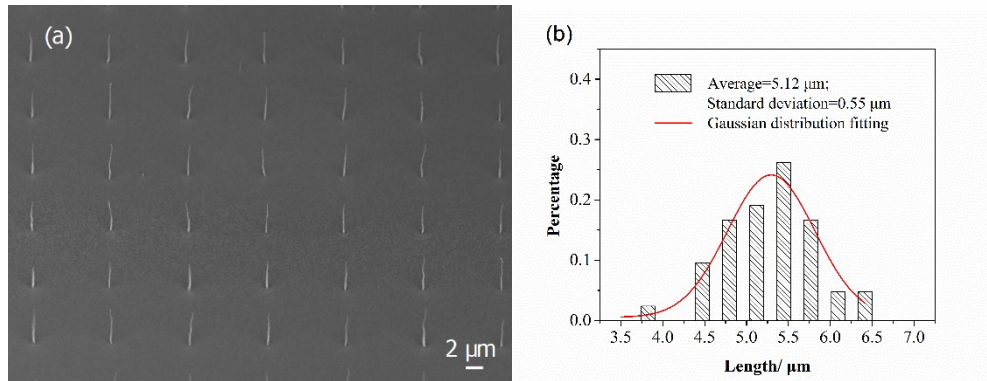


Fig. S1 (a) A typical CNF field emitter array (FEA) using the same synthesis process as the 11×11 CNF FEA. (b) Distribution in CNF emitters' heights and Gaussian distribution fitting. The CNF emitters have an average height of 5.12 μm and a standard deviation of 0.55 μm, which is 10.7% of the average.

2. Experimental validation of CNF explosion

FE test using a 10×10 CNF FEA under the same conditions is performed. The difference is that there is no PMMA thin film on the indium tin oxide coated glass and the anode-cathode gap is 50 μm. Explosions at five CNF emission sites are directly observed using the microscopic camera during a scanning voltage FE test from 300 V to 800 V with 5 V step. Among the five exploded sites, site D-5 is found exploded when the scanning voltage is from 200 V to 700 V of the previous run. Fig. S2(a) shows the video screen-shot after five explosions. Take site D-8 as an example. Fig. S2(b) and (c) show the video screen-shot of the site D-8 before and after the explosion occurs, respectively. Fig. S2(d) shows the optical microscopic image of the anode surface. Except for some particles, no other debris are found on the anode surface. Melted area and explosion craters are also found at the site D-8 on the substrate by scanning electron microscopy (SEM) (Fig. S2(e)), indicating a history of high temperature and explosion. Since there is no PMMA thin film on the anode surface, no explosion debris is found around the melted area and explosion craters. The clean substrate surface in return proves that the explosion debris in the 11×11 CNF FEA are sputtered PMMA. Besides, the explosion events themselves are not as visually impressive as those with PMMA thin film on the anode surface. This experiment confirms that it is the CNF emitters rather than PMMA thin film that explode. The damaged PMMA thin film and explosion debris around the explosion sites are caused by CNF explosion.

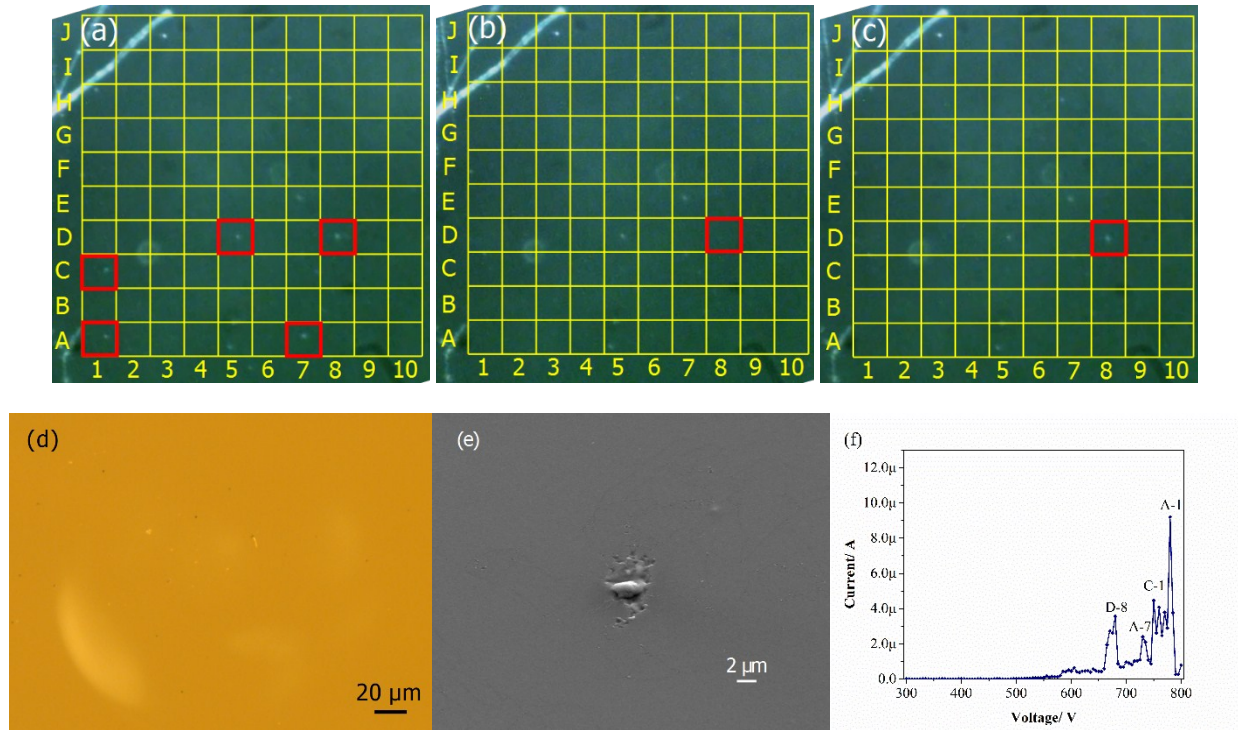


Fig. S2 Experimental validation of CNF emitter explosion: (a) video screen-shot after five explosions; (b) video screen-shot before explosion occurs at site D-8; (c) video screen-shot of explosion at site D-8. Due to no PMMA on the anode surface, the explosion is not as visually impressive as that with PMMA thin film on the anode surface. (d) Optical microscopic image of the anode surface at site D-8. (e) SEM image of damaged substrate at the explosion site D-8. Melted area can be clearly identified. There is no debris found on the substrate surface around the explosion site. (f) I-V curve of the CNF FEA. The impact of the four explosion sites on the FE current can be seen.

3. Energy-dispersive X-ray spectroscopy analysis of the explosion site

Energy-dispersive X-ray spectroscopy (EDS) is used to verify that both Joule heating and explosion occur during the CNF emitter failure. The substrate is silicon with a thin layer of TiN of 70 nm on top. CNF is synthesized on TiN layer. Thus Si, Ti, N, and C are the four elements detected. Fig. S3(a) shows the SEM image of a typical explosion site I-3. The EDS analysis is conducted on the explosion center, explosion debris, and intact TiN surface of the site, corresponding to spectrum 1, 2, and 3 (Fig. S3(b)), respectively.

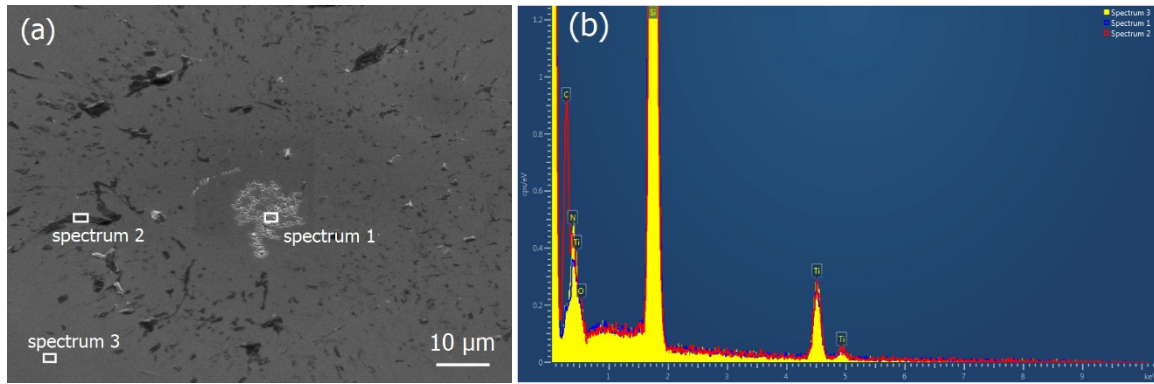


Fig. S3 EDS analysis of a typical CNF emitter explosion site I-3: (a) the explosion center, the explosion debris, and the intact TiN surface. The SEM image is taken at a tilted angle of 45°. (b) Comparison among spectrum 1, spectrum 2, and spectrum 3. Spectrum 1 has the highest peak of Si but lowest peak of N. Spectrum 2 has the highest peak of C but lowest peak of Si.

Table S1 show the four elements content variation in the three areas.

Table S1. EDS analysis of atomic percentage of each element from the three spectrums.

Element	Line type	Atomic percentage from	Atomic percentage from	Atomic percentage from
		spectrum 1	spectrum 2	spectrum 3
C	K series	22.51	53.65	20.12
N	K series	7.84	10.09	15.64
O	K series	3.65	3.64	2.88
Si	K series	57.32	24.96	48.08
Ti	K series	8.67	8.66	13.28

The TiN layer deposited by reactive sputter has an extended range of composition (TiN_x with $0.6 < x < 1.5$).¹ The atomic percentage ratio of N to Ti of the intact TiN surface is about 1.17, which is calculated from spectrum 3. However, compared with the other two spectrum, spectrum 1 has the most atomic percentage of Si but the least atomic percentage of N, which means that in the explosion center TiN layer is damaged and silicon substrate exposes. Spectrum 2 has the most atomic percentage of C. Considering such an amount of explosion remains on the substrate and PMMA chemical formula that is $(\text{C}_5\text{O}_2\text{H}_8)_n$, we believe these explosion remains contain not only CNF fragments but also PMMA from the anode surface. The atomic percentage ratio of Ti & N to Si in spectrum 2 and spectrum 3 are almost the same. This result indicates that the substrate under the explosion debris is intact. Therefore, EDS results verify that Joule heating of CNF emitters melts the contact area and exposes the substrate around the contact area.

4. Tubular cone structure of CNF emitters

Vertically aligned CNF FEA is fabricated by plasma enhanced chemical vapor deposition (PECVD) of acetylene and ammonia at 700 °C at precisely positioned nickel catalyst dots.²⁻⁶ In the CNF FEA, each patterned catalyst site has a single vertically aligned CNT emitter with well-controlled size and a tubular conical structure. The CNT emitters consist of stacked curved graphite layers that form tubular cones with bamboo-type axial.^{7, 8} TEM images also reveal that the graphene layers are formed parallel to the substrate near the base of PECVD CNF and subsequent layer edges bend upward as a cone-like structure.⁹ Such a structure of CNF can be verified by our mechanically damage CNFs on the marker with a typical CNF lying beside, shown in Fig. S4.

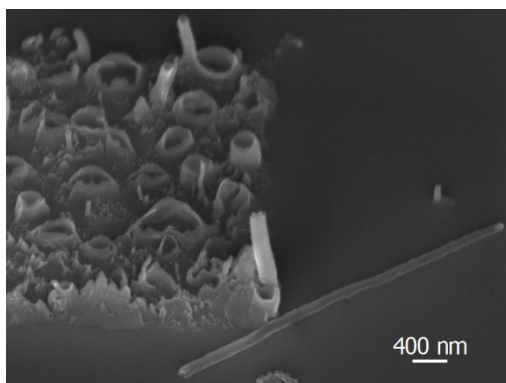


Fig. S4 Mechanically damaged CNFs on the marker with a typical CNF lying beside, showing a tubular cone structure of the CNF.

5. Supplementary videos

Supplementary video S1 shows the full process of the 11×11 CNF FEA during FE tests. Light emissions and explosions can be seen. The video is 50 times fast forward.

Supplementary video S2, S3, and S4 shows the light emission and explosion of the CNF emitter at site A-2, F-5, and G-9, respectively. The supplementary video S2 and S4 are at a normal speed. While the supplementary video S5 is 10 times fast forward due to a long period of light emission occurring, reoccurring and explosion.

References

1. N. Savvides and B. Window, *J. Appl. Phys.*, 1988, **64**, 225-234.
2. Z. F. Ren, Z. P. Huang, J. W. Xu, J. H. Wang, P. Bush, M. P. Siegal and P. N. Provencio, *Science*, 1998, **282**, 1105-1107.
3. Z. Ren, Z. Huang, D. Wang, J. Wen, J. Xu, J. Wang, L. Calvet, J. Chen, J. Klemic and M. Reed, *Appl. Phys. Lett.*, 1999, **75**, 1086-1088.

4. K. Teo, S. Lee, M. Chhowalla, V. Semet, V. T. Binh, O. Groening, M. Castignolles, A. Loiseau, G. Pirio and P. Legagneux, *Nanotechnology*, 2003, **14**, 204.
5. M. Chhowalla, K. Teo, C. Ducati, N. Rupesinghe, G. Amaratunga, A. Ferrari, D. Roy, J. Robertson and W. Milne, *J. Appl. Phys.*, 2001, **90**, 5308-5317.
6. Y. Li, Y. Sun and J. Yeow, *Nanotechnology*, 2015, **26**, 242001.
7. A. V. Melechko, V. I. Merkulov, T. E. McKnight, M. Guillorn, K. L. Klein, D. H. Lowndes and M. L. Simpson, *J. Appl. Phys.*, 2005, **97**, 041301.
8. M. Meyyappan, *J. Phys. D*, 2009, **42**, 213001.
9. H. Cui, X. Yang, M. L. Simpson, D. H. Lowndes and M. Varela, *Appl. Phys. Lett.*, 2004, **84**, 4077-4079.